JOURNAL OF VIROLOGY, Nov. 2003, p. 11952–11963 Vol. 77, No. 22
0022-538X/03/$08.00+0 DOI: 10.1128/JVI.77.22.11952–11963.2003

Induction of Caspase-Dependent Apoptosis in Cultured Rat Oligodendrocytes by Murine Coronavirus Is Mediated during Cell Entry and Does Not Require Virus Replication

Yin Liu, Yingyun Cai, and Xuming Zhang*

Department of Microbiology and Immunology, University of Arkansas for Medical Sciences, Little Rock, Arkansas 72205

Received 2 May 2003/Accepted 12 August 2003

Murine coronavirus mouse hepatitis virus (MHV) causes demyelination of the central nervous system (CNS) in rats and mice. Apoptotic oligodendrocytes have been detected in the vicinity of the CNS demyelinating lesions in these animals. However, whether MHV can directly induce oligodendrocyte apoptosis has not been documented. Here, we established a rat oligodendrocyte culture that is morphologically and phenotypically indistinguishable from the primary rat oligodendrocytes. Using this culture, we showed that mature rat oligodendrocytes were permissive to MHV infection but did not support productive virus replication. Significantly, oligodendrocytes infected with both live and ultraviolet light-inactivated viruses underwent apoptosis to a similar extent, which was readily detectable at 24 h postinfection as revealed by apoptotic bodies and DNA fragmentation, indicating that MHV-induced apoptosis is mediated during the early stages of the virus life cycle and does not require virus replication. Prior treatment of cells with the lysosomotropic agents NH_4Cl and chloroquine as well as the vacuolar proton pump-ATPase inhibitor bafilomycin A1, all of which block the acidification of the endosome, prevented oligodendrocytes from succumbing to apoptosis induced by MHV mutant OBLV60, which enters cells via endocytosis, indicating that fusion between the viral envelope and cell membranes triggers the apoptotic cascade. Treatment with the pan-caspase inhibitor Z-VAD-fmk blocked MHV-induced apoptosis, suggesting an involvement of the caspase-dependent pathway. Our results, thus, for the first time provide unequivocal evidence that infection of oligodendrocytes with MHV directly results in apoptosis. This finding provides an explanation for the destruction of oligodendrocytes and the damage of myelin sheath in MHV-infected CNS and suggests that oligodendrocyte apoptosis may be one of the underlying mechanisms for the pathogenesis of MHV-induced demyelinating diseases in animals.

Apoptosis is a genetically programmed, morphologically distinct form of cell death that is involved in the regulation of homeostasis, tissue development, and the immune system by eliminating cells that are no longer useful. Apoptosis also functions by eliminating aberrant cells created by DNA damage or those infected by viruses. Survival factors prevent normal cells from succumbing to apoptosis, but upon receipt of a variety of apoptotic signals, including DNA damage, virus infection, and toxic insults, death pathways are initiated (35, 38). Cell death by apoptosis is characterized by chromatin condensation, plasma membrane blebbing, cell shrinkage, and DNA fragmentation into membrane-enclosed vesicles or apoptotic bodies (50). Successful viral replication requires not only the efficient production and spread of progeny but also evasion of host defense mechanisms that limit replication by killing infected cells. Thus, apoptosis can also be a viral strategy to enhance the spread of progeny to neighboring cells. In addition to inducing immune and inflammatory responses, infection by many viruses triggers apoptosis of the infected cell. For example, the E1A protein of adenovirus can induce sensitivity to tumor necrosis factor (11, 12, 32); the Tax of human T-cell leukemia virus can increase Fas ligand synthesis (5). These viruses induce apoptosis through activating the caspases via the death receptors of the tumor necrosis factor receptor superfamily. On the other hand, many viruses have also devised powerful weapons to counteract apoptosis. These antiapoptotic measures are likely beneficial to virus survival in its host, for apoptosis results in elimination of its host and thereby its own very existence. For example, the human immunodeficiency virus tat protein inhibits apoptosis by inducing the expression of the antiapoptotic protein Bcl-2 (8). Thus, many viruses have evolved mechanisms to induce apoptosis or to cope with the cellular antiviral and apoptotic responses.

Murine coronavirus mouse hepatitis virus (MHV) is a single-strand, positive-sense RNA virus that consists of an outer envelope and an inner nucleocapsid core. The envelope contains three to four proteins depending on virus strains: the spike (S) glycoprotein is responsible for attachment of the virus to the receptors of permissive cells, fusion between viral envelope and cell membrane during virus entry, and elicitation of neutralizing antibodies and cellular immune responses (6, 25, 42). Thus, the S protein is essential for viral infectivity. The hemagglutinin/esterase (HE) glycoprotein is present only in certain MHV strains such as JHM; it is not required for virus entry (51, 52). The membrane glycoprotein (M) and the small envelope (E) protein are embedded in the envelope and are essential for virion envelopment and assembly (34, 45, 55). The nucleocapsid (N) protein is a phosphorylated protein that is associated with the viral RNA genome to form the nucleocapsid (41). Infection of host cells is initiated by the interaction between virion S protein and the cell receptors, which then

* Corresponding author. Mailing address: Department of Microbiology and Immunology, University of Arkansas for Medical Sciences, 4301 W. Markham St., Slot 511, Little Rock, AR 72205-7199. Phone: (501) 686-7415. Fax: (501) 686-5359. E-mail: zhangxuming@uams.edu.

triggers the fusion between viral envelope and plasma membrane or endosomal membrane, the latter of which follows receptor-mediated endocytosis. The cellular receptors for MHV are the members of the carcinoembryonic antigen family of the immunoglobulin superfamily (13, 47, 53). MHV enters cells by fusion with plasma and endosomal membranes (24, 33). Following fusion, it is believed that MHV uncoating is initiated via dephosphorylation of the N protein and subsequent separation of the N protein from genomic RNA (22) such that the viral genomic RNA is ready for translation of the viral RNA-dependent RNA polymerase.

Rodents are the natural hosts for MHV. MHV infects rodents and causes hepatitis, nephritis, enteritis, and central nervous system (CNS) diseases, including encephalitis and demyelination. Because the histopathology of the MHV-induced CNS demyelinating disease in rodents resembles that seen in human multiple sclerosis patients (26), MHV has been extensively used as an animal model for studying the pathogenesis of multiple sclerosis and other neurodegenerative diseases. Following intracerebral inoculation with MHV, mice first develop acute encephalitis and demyelination. Demyelination can be observed as early as 6 days postinfection (p.i.) and appears most extensive at around 4 weeks p.i., at which time infectious virus can no longer be isolated although viral RNA is still detectable (10, 23, 27). The mechanism of MHV-induced demyelination is unclear, although both macrophages and T cells have been implicated as mediators of the pathological changes (48, 49). Lymphocyte-deficient severe combined immunodeficiency (SCID) mice, recombinase-activating gene 1 (RAG-1) knockout mice, and UV-irradiated mice infected with MHV strain JHM hardly have lesions 7 to 15 days p.i., despite high levels of virus replication (14, 19, 46, 49). These data suggest that lymphocytes are required for robust acute demyelination (29, 30). Reconstitution studies suggest that $CD4^+$ or $CD8^+$ T cells can mediate MHV-JHM-induced demyelination (49). However, in nude mice that lack $CD4^+$ and $CD8^+$ T cells, demyelination still occurs (19), which has been shown recently to be mediated by γδ T cells (9). A recent study showed, however, that demyelination occurred to a similar extent in wild-type, B-cell-deficient, and RAG1 knockout mice and in mice lacking antibody receptors or complement pathway activity when infected with MHV strain A59 (29). Thus, although the immune system may play a role in acute demyelination, it appears that in the absence of an intact immune response, MHV infection in the CNS is directly responsible for the onset of demyelination, probably through the destruction of oligodendrocytes (29). Apoptotic oligodendrocytes have been detected in and near the demyelinating lesions in the CNS of mice and rats infected with MHV JHM and A59 (2, 39, 48). However, whether oligodendrocyte apoptosis results from direct viral infection or from indirect attack by inflammatory molecules secreted from neighboring cells of virus-infected CNS and from infiltrated cells is not clear.

In the present study, we determined whether MHV is capable of inducing apoptosis in cultured rat oligodendrocytes. Our results showed that rat oligodendrocytes were susceptible to MHV infection, as virions were internalized into the cells but did not support productive viral replication. Significantly, rat oligodendrocytes underwent apoptosis following infection with both live and UV-inactivated MHV, indicating that the apoptosis was triggered during early steps of the virus life cycle that are prior to viral RNA synthesis. Furthermore, MHV-induced apoptosis in oligodendrocytes appeared to be mediated via caspases, since it was completely inhibited by the pan-caspase inhibitor Z-VAD-fmk. Our results thus provide unequivocal evidence that MHV infection can directly result in oligodendrocyte apoptosis. Our data suggest that oligodendrocyte apoptosis may be one of the underlying mechanisms for the pathogenesis of MHV-induced demyelinating diseases in animals.

MATERIALS AND METHODS

Cells, viruses, and reagents. The central glial CG-4 cell is a permanent, undifferentiated type 2 oligodendrocyte/astrocyte progenitor cell that was originally established during a primary neural cell culture derived from the brain of newborn Sprague-Dawley rat pups (1 to 3 days postnatal) (28). It was kindly provided by Paul Drew (University of Arkansas for Medical Sciences). CG-4 cells were cultured on poly-L-ornithine (0.1 mg/ml)-coated dishes at a seeding density of 100 cells per mm^2 in serum-free Dulbecco minimum essential medium (DMEM) with the N1 supplement (5 μg of transferrin/ml, 16.11 μg of putrescine/ml, 6.29 ng of progesterone/ml, 5.14 ng of selenium/ml), biotin (10 ng/ml), insulin (5 μg/ml), and two growth factors (basic fibroblast growth factor 2 at 5 ng/ml and platelet-derived growth factor AA at 10 ng/ml) and streptomycin and penicillin. CG-4 cells were passaged every 6 days. Under this condition, the CG-4 cell maintains its undifferentiated progenitor phenotype indefinitely. Withdrawal of the two growth factors inhibits proliferation and promotes differentiation into either oligodendrocytes or type 2 astrocytes. In the presence of a low concentration of serum (≤0.5%), it differentiates into an oligodendrocyte. Differentiated oligodendrocytes can survive for 2 to 3 weeks in the differentiating medium. Therefore, for maintenance the progenitor cells were cultured continuously, while differentiated oligodendrocytes were used for virus infection throughout this study. Mouse astrocytoma DBT cells (17) were cultured in MEM and were used for virus propagation and plaque assays.

MHV strain JHM was used throughout this study. For some experiments, the pH-dependent mutant OBLV60 was used, which was kindly provided by Michael Buchmeier (Scripps Research Institute, La Jolla, Calif.). This mutant was originally isolated from the olfactory bulb of mice persistently infected with JHM (15). All MHVs were propagated in DBT cells. The broad-range caspases inhibitor Z-Val-Ala-Asp-fmk (Z-VAD-fmk) was purchased from MD Biosciences, Division of Morwell Diagnostics GmbH (Zurich, Switzerland). A stock solution of 100 mM was made in water and stored in a −20°C freezer.

Immunocytochemistry. For immunostaining, progenitor CG-4 cells and differentiated oligodendrocytes were grown on four-well chamber slides (Nalgene) in respective culture media, fixed with 4% paraformaldehyde for 10 min at room temperature, and permeabilized with 1% Triton X-100 for 30 min. Cells were then stained with a mouse monoclonal antibody (MAb) specific to A2B5 (a marker protein for the progenitor cells) or rat MAb specific to the myelin basic protein (MBP) (a marker for mature oligodendrocytes) for 90 min at 37°C followed by incubation with a fluorescein isothiocyanate (FITC)-conjugated goat anti-mouse or goat anti-rat immunoglobulin G antibody (Sigma). Both anti-A2B5 and anti-MBP MAb's were purchased from Chemicon International, Inc. For detection of MHV protein expression, the MAb specific to the MHV N protein (kindly provided by Stephen Stohlman, USC Keck School of Medicine) was used. The routine immunocytochemistry method was used in this study. The stained cells were observed under a fluorescence microscope (Olympus IX-70), and photographs were taken with the attached digital camera (MagnaFire).

Propagation, purification, and radiolabeling of viruses. For virus propagation, DBT cells were infected with MHV strains at a multiplicity of infection (MOI) of 1 and incubated overnight. Culture medium and cell lysates were collected following freezing and thawing once and clarifying of cell debris by centrifugation at 3,000 × *g* for 30 min at 4°C (Marathon 3200R; Fisher Scientific). For virus purification, clarified virus preparation was loaded onto a 30% (wt/vol) sucrose cushion and centrifuged at 27,000 rpm for 3 h at 4°C in an SW27/28 rotor (Beckman). Supernatants were discarded; the pellets that contained the virus were resuspended in phosphate-buffered saline (PBS), loaded onto a 20 to 70% (wt/vol) sucrose step gradient, and centrifuged at 35,000 rpm for 16 h at 4°C in an SW41 rotor (Beckman). The fractions that correspond to viral buoyant density were collected. Following dilution in PBS, viruses were pelleted by centrifugation at 35,000 rpm for 1 h at 4°C in an SW41 rotor (Beckman). Pelleted virus was resuspended in either PBS or serum-free medium. For virus labeling, DBT

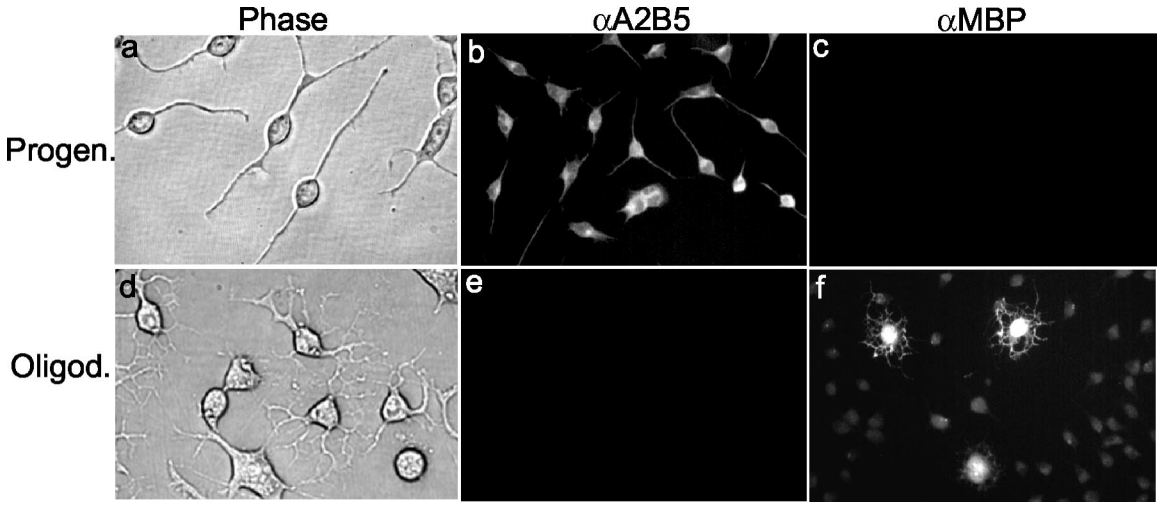

FIG. 1. Morphological and biochemical properties of the undifferentiated CG-4 progenitor cells and the differentiated oligodendrocytes. (a to c) Progenitor cells were cultured in the undifferentiating medium as described in Materials and Methods. (d to f) Mature oligodendrocytes were differentiated from progenitor cells for more than 48 h in the differentiating medium (see Materials and Methods). Panels a and d are phase-contrast microscopic images of the cell cultures. Panels b and e and c and f show immunofluorescence staining results with the primary monoclonal antibodies to A2B5 (a marker for progenitor cells) and MBP (a marker for mature oligodendrocytes), respectively, and the secondary antibodies conjugated with FITC. Cells were observed under the microscope (Olympus IX-70), and all images were taken with the attached digital camera (MagnaFire).

cells were grown to confluency in a 60-mm petri dish and were infected with MHV at an MOI of 10. At 1 h p.i., actinomycin D was added to the medium at a concentration of 10 μg per ml. At 2 h p.i., [^{3}H]uridine was added to the culture at 100 μCi per ml. Radiolabeled virus was collected and purified as described above. Radioactivity was determined by liquid scintillation counting (model T2500; Beckman). Virus titers were determined by standard plaque assay in DBT cells as described previously (18).

Virus internalization assay. For the virus internalization assay, CG-4 cells were differentiated into oligodendrocytes and were grown on 60-mm dishes to subconfluency in the differentiation medium. ^{3}H-labeled and sucrose gradient-purified viruses were then used to infect differentiated oligodendrocytes. The virus internalization assay was performed as described previously (44). Briefly, cells were infected with MHV-JHM at an MOI of 10 at 4°C for 1 h. Unbound virus was then removed by washing five times with PBS containing 0.5% bovine serum albumin (BSA) and 0.05% Tween 20. Infected cells were incubated at 37°C. At 45 min following temperature shift, infected cells were washed with cold PBS and incubated with 0.5 mg of proteinase K/ml at 4°C for 45 min to remove the bound but uninternalized virus particles. Cells were collected with a rubber scraper, mixed with an equal volume of a buffer containing 2 mM phenylmethylsulfonyl fluoride and 6% BSA to inactivate proteinase K, and centrifuged for 30 s at 14,000 rpm in a microcentrifuge (Micromax). Cell pellets were washed with MEM containing 2% BSA. Cells were then resuspended in MEM, and an equal volume of a solution containing 1% sodium dodecyl sulfate and 10% trichloroacetic acid was added to precipitate the radiolabeled nucleic acids. The radioactivities in the precipitable materials were determined by liquid scintillation counting (model T2500; Beckman). Parallel experiments were performed on DBT cells, which were used as a positive control. Three replicas per sample were analyzed.

UV inactivation of viruses. To inactivate the virus by UV light, purified virus was diluted to a concentration of 10^7 PFU per ml in serum-free medium. Aliquots of 1 ml were added to each well of the six-well tissue culture plate. The plates were placed on ice at a distance of 14 cm from the UV light in a UV Cross-linker (Fisher Scientific) and exposed to UV light at energy of 120 mJ/cm^2 for 30 min. Viral inactivation was confirmed by titration of samples before and after UV exposure and by the absence of cytopathic effect (CPE) after inoculation of DBT cell monolayers with the UV-irradiated virus samples. Preliminary experiments indicated that a 10-min exposure to such UV light completely inactivated MHV infectivity.

Detection of subdiploid cell populations. Apoptotic nuclei containing subdiploid DNA content were determined by propidium iodide staining and flow cytometric analysis as described previously (54). Briefly, at various time points, adherent and floating cells were collected and centrifuged at 1,000 × *g* for 5 min. Pelleted cells were resuspended in PBS, centrifuged, and then fixed with 70% ice-cold ethanol and incubated overnight at 4°C. Cells were centrifuged, resuspended in PBS, and incubated with 50 μg of propidium iodide/ml and 100 μg of RNase A (Sigma)/ml. Aliquots of 10^6 cells were subjected to flow cytometric analysis with a FACSCalibur flow cytometer equipped with an argon ion laser (488 nm), and the data were acquired and analyzed with CELLQuest software (Becton Dickinson).

DNA fragmentation assay. For DNA fragmentation analysis, oligodendrocytes were grown to subconfluency at approximately 10^6 cells per 60-mm petri dish and were infected or mock infected with MHV at an MOI of 10. At a 24-h interval p.i., cells were harvested from the dish by scraping with a rubber policeman and low-speed centrifugation (1,000 × *g*). Cell pellets were lysed with a lysis buffer, and total cellular DNAs were then extracted using the Suicide-track DNA ladder isolation kit according to the manufacturer's recommended procedure (CN Biosciences, Inc.). DNAs were analyzed by 1.5% agarose gel electrophoresis and visualized by staining with ethidium bromide.

RESULTS

Characterization of the progenitor CG-4 cells and mature oligodendrocytes. The morphological, biochemical, and biological properties of the progenitor CG-4 cells have been well characterized previously (28, 31). To ensure that the CG-4 cell has maintained its progenitor phenotype upon continuous cultivation in our laboratory, we employed microscopic and immunocytochemistry methods. We found that in the continuous presence of both growth factors (basic fibroblast growth factor 2 and platelet-derived growth factor) in the medium, CG-4 cells maintained their undifferentiated, progenitor morphology, i.e., the majority of the cells contained bipolar processes with a few cells having short and relatively unbranched multipolar processes (Fig. 1a). These cells were stained with an antibody specific to A2B5, a molecular marker for progenitor cells (Fig. 1b). In contrast, they could not be stained with an antibody specific to MBP, a later marker for mature oligodendrocytes (Fig. 1c). When the CG-4 cells were cultured in the medium containing less than 0.5% of fetal calf serum without

the two growth factors for more than 2 days, more than 98% of the cells differentiated and acquired a phenotype typical of oligodendrocytes, which are characterized by numerous long branched processes (Fig. 1d) and positive staining with the antibody specific to MBP (Fig. 1f), but not with the anti-A2B5 antibody (Fig. 1e). Differentiated oligodendrocytes could no longer be subcultured and died in 2 to 3 weeks in the differentiation medium, confirming the terminal differentiation phenotype for mature oligodendrocytes. These data thus establish that the CG-4 cells maintained their progenitor phenotype.

Oligodendrocytes are susceptible to MHV infection, but they do not support productive viral replication. Previous studies on primary rat oligodendrocytes have suggested that oligodendrocytes are susceptible to MHV infection only for a very short period of time during differentiation; once fully differentiated, they become resistant to MHV infection (36). The resistance was found to occur in the cytoplasm after virus entry but prior to virus uncoating, most likely due to the inhibition of dephosphorylation of the viral nucleocapsid protein (22). To determine whether mature oligodendrocytes differentiated from the progenitor CG-4 cells are susceptible to MHV infection, we infected mature oligodendrocytes with MHV-JHM at an MOI of 10. At various time points p.i., we observed the cell morphology under a light microscope and determined the production of infectious virus by plaque assay. We found that most virus-infected cells manifested CPE, i.e., shrinkage, rounding, and detachment from the plate (data not shown), whereas mock-infected cells showed the normal, typical multipolar morphology of oligodendrocytes, indicating that mature oligodendrocytes are susceptible to MHV infection. Consistent with the observation of Beushausen et al. (3), we found that virus titers decreased substantially and sequentially (approximately 1 log reduction per 24-h period) from 24 to 96 h p.i. (Fig. 2A). These results demonstrate that mature oligodendrocytes do not support productive virus replication.

To ensure that the mature oligodendrocytes were indeed infected by MHV and that the failure of virus production was not due to a block of virus entry, we performed a virus internalization assay. Mature oligodendrocytes were infected with [^{3}H]uridine-labeled virus at an MOI of 10 for 1 h at 4°C. Unbound virus was removed, and bound virus was allowed to penetrate following temperature shift from 4 to 37°C. Virus that was bound to the cell surface but was not internalized into the cell was then removed by treatment with proteinase K. Radioactivity detected from lysates of cells that were treated with proteinase K and extensively washed with a buffer would be indicative of virus internalization. As shown in Fig. 2B, significant radioactivity was detected in oligodendrocytes infected with MHV-JHM at 37°C, indicating that the virus had entered into the cell. This entry appeared to be specific, because no radioactivity was detected in lysates of cells that were adsorbed with the radiolabeled virus at 4°C without temperature shifting to 37°C. In a parallel experiment, the radioactivities in oligodendrocyte lysates were comparable to those obtained in DBT cells, which is a permissive cell line routinely used for MHV propagation.

As an alternative approach to verify the infectious process, we performed a one-step growth curve experiment. Cells were infected with MHV-JHM at an MOI of 10. At various time points p.i., cultures were collected and virus titers were determined by plaque assay. Indeed, virus titers were reduced to 10^5 PFU/ml (2 log reduction) at 2 h p.i. and maintained at a similar level by 4 h p.i.; virus titers began to increase slightly at 4 h p.i. and reached a plateau of 3×10^6 PFU/ml at 6 h p.i. Thereafter, the virus titers began to drop slightly to 2×10^6 PFU/ml at 8 h p.i. (Fig. 2C). The small increase (more than 1 $\log_{10}$) in virus titer following the eclipse period suggested that MHV did replicate in this oligodendrocyte culture, albeit poorly.

Two potential scenarios might have contributed to the low virus yield. One is that the replication of the infected virus was very slow in this cell culture, and the other is that only a small population of the cells supported virus replication. To distinguish these two possibilities, we monitored the virus gene expression by performing fluorescence staining with a MAb against the most prominent viral N protein. If the former is the case, we would be able to detect an overall weak staining of the N protein; if the latter is the contributing factor, then we would detect a few cells with strong fluorescence staining. The results showed that less than 1% of the cells exhibited strong fluorescence staining, which resided within the fusion foci (Fig. 2D), although the staining was comparatively much weaker than in DBT cells (data not shown). These results favor the notion that the low virus yield in the oligodendrocyte culture was likely due to a limited number of cells that supported MHV replication. The identity of these fluorescent cells was not determined, although they appeared to be undifferentiated CG-4 cells morphologically (Fig. 2D). Taken together, we conclude that mature oligodendrocytes are susceptible to MHV-JHM infection but do not support productive virus replication.

MHV infection induced apoptosis in cultured oligodendrocytes. Since infected oligodendrocytes exhibited CPE, which resembles the morphology of apoptotic cells and which has not been well documented in the literature, we were interested in examining whether MHV infection induces apoptosis or necrosis in rat mature oligodendrocytes. To address this question, we infected the mature oligodendrocytes with MHV-JHM at an MOI of 10 and examined the virus-infected oligodendrocytes every 24 h from 24 to 96 h p.i. for different biochemical hallmarks of apoptosis. We first stained the nuclei of infected oligodendrocytes with propidium iodide and then observed the nuclear structure under a fluorescence microscope. As shown in Fig. 3, infected oligodendrocytes exhibited nuclear damage with chromatin condensation, margination, and broken nuclei beginning at 24 h p.i. and peaking at 72 to 96 h p.i., whereas mock-infected cells had intact nuclei throughout the 96-h period. To provide a quantitative assessment on the extent of apoptosis, cells were examined by flow cytometry following staining with propidium iodide. The results showed that a small percentage (13.7 to 20.2%) of the uninfected cells displayed a sub-G_0/G_1 DNA content at 24 to 96 h p.i., respectively (Fig. 3B, top row labeled Mock). In contrast, a significantly higher percentage (23.5 to 71.2%) of MHV-infected oligodendrocytes shifted to sub-G_0/G_1 phase for the same time points p.i. (Fig. 3B, middle row labeled Virus). To ascertain further that these sub-G_0/G_1-phase cells indeed resulted from apoptosis and not from necrosis, we infected oligodendrocytes with MHV-JHM at an MOI of 10 and isolated cellular DNAs at various time points p.i. for DNA fragmentation analysis. Consistent with the results from propidium iodide staining and flow cytometric analysis, internucleosomal DNA fragmentation into an oligo-

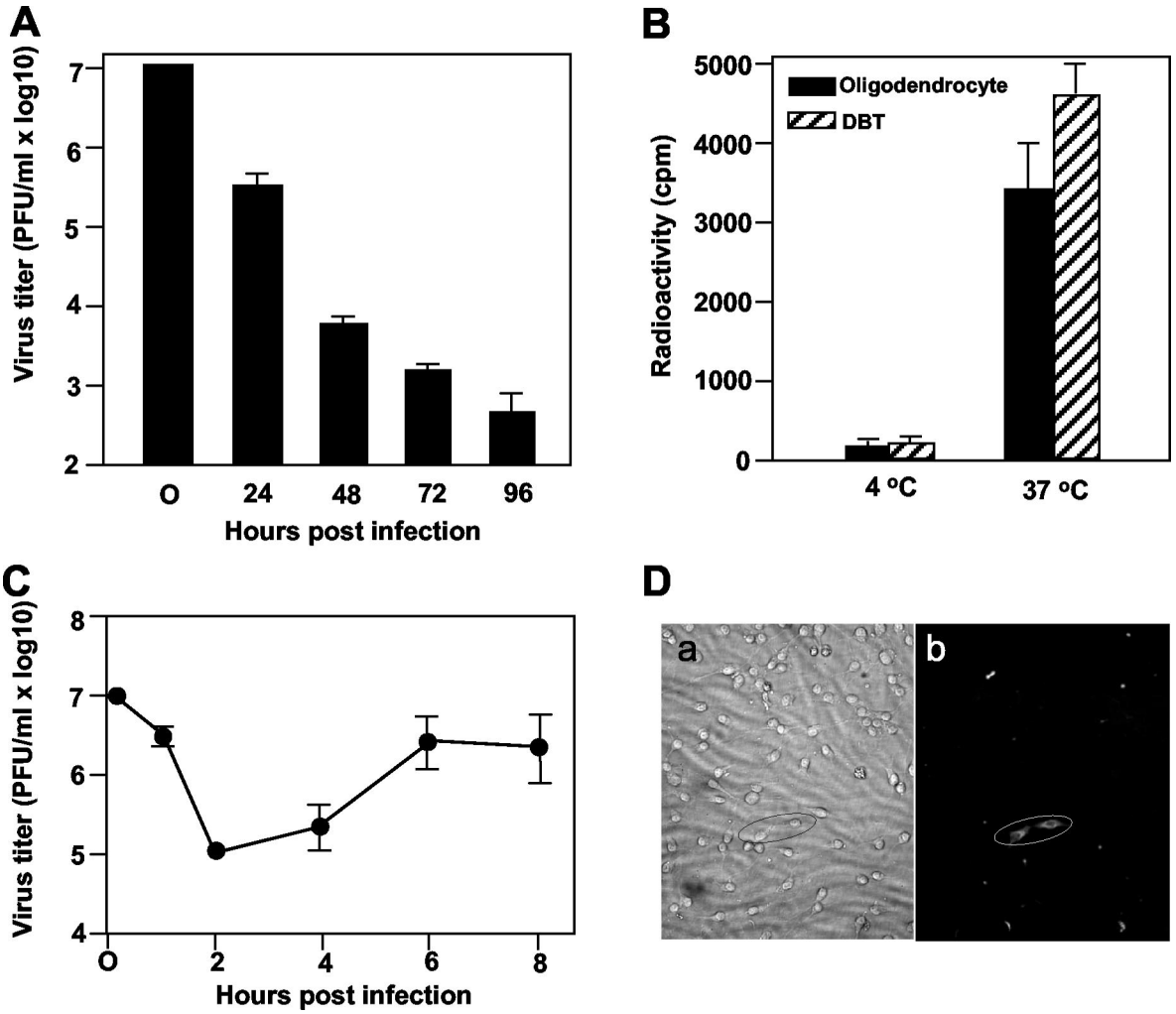

FIG. 2. MHV replication in mature rat oligodendrocytes. (A) Characteristics of MHV replication in oligodendrocytes. CG-4 progenitor cells were allowed to differentiate into oligodendrocytes for at least 48 h in the differentiation medium. Mature oligodendrocytes (approximately 10^6 cells) were infected with MHV strain JHM at an MOI of 10. At each time point p.i. as indicated, virus titers recovered from the oligodendrocyte cultures were determined by plaque assay in DBT cells. The results are expressed as the mean PFU per milliliter for three independent experiments. Error bars indicate standard deviations of the means. The virus titer at 0 h p.i. denotes the virus titer for the inoculum. (B) Internalization of MHV into mature oligodendrocytes during infection. MHV strain JHM was grown in DBT cells, and the virus genomic RNAs were labeled with [^{3}H]uridine as described in Materials and Methods. Radiolabeled virus was then purified through sucrose gradient ultracentrifugation and was used for infection of oligodendrocytes. Infection of DBT cells, which are permissive for MHV infection, was used as a positive control. Virus attachment was carried out at 4°C for 1 h. Following extensive washing of unbound viruses, one set of cell cultures was moved to 37°C for an additional hour to allow internalization. The other set of cultures remained at 4°C for an additional hour. At the end of the second hour, bound but uninternalized virus was removed by treatment with protease K. Cells were then lysed, and intracellular radioactivities were determined in a liquid scintillation counter. Results are expressed as the mean counts per minute for three independent experiments. Error bars indicate standard deviations of the means. (C) One-step growth curve. The experiment was performed as for panel A except that the virus titers were determined at earlier time points p.i. (D) Detection of viral proteins by immunofluorescence assay. Mature oligodendrocytes were infected with MHV strain JHM at an MOI of 10. At approximately 24 h p.i., cells were stained with a MAb specific to MHV N protein and a second anti-mouse immunoglobulin G antibody conjugated with FITC. Stained cells were observed under the microscope (Olympus IX-70). Images of both phase contrast (a) and fluorescence staining (b) for the same field were taken with an attached digital camera (MagnaFire). Two specifically stained fluorescent cells are circled. Note that other fluorescent spots are nonspecific fluorescence of cell debris.

nucleosome-length DNA ladder was evident in virus-infected cells from 24 to 96 h p.i. (Fig. 4, Virus lanes) but not in mock-infected cells (Fig. 4, Mock lanes). It is noted that in all of the above experiments we used virus inoculum that was purified through sucrose-gradient ultracentrifugation and was devoid of cultured medium. Therefore, any effect on oligodendrocytes observed during virus infection must be virus specific and not the effect of soluble factors secreted from DBT cells into the medium during virus propagation. Taken together, these results establish that MHV infection induced apoptosis in mature rat oligodendrocytes.

Apoptosis of cultured oligodendrocytes is triggered during an early stage of virus infection and does not require virus replication. To determine which specific step(s) of the virus life cycle is responsible for the apoptosis induction, we inactivated the virus with UV light. It is known that UV-inactivated virus

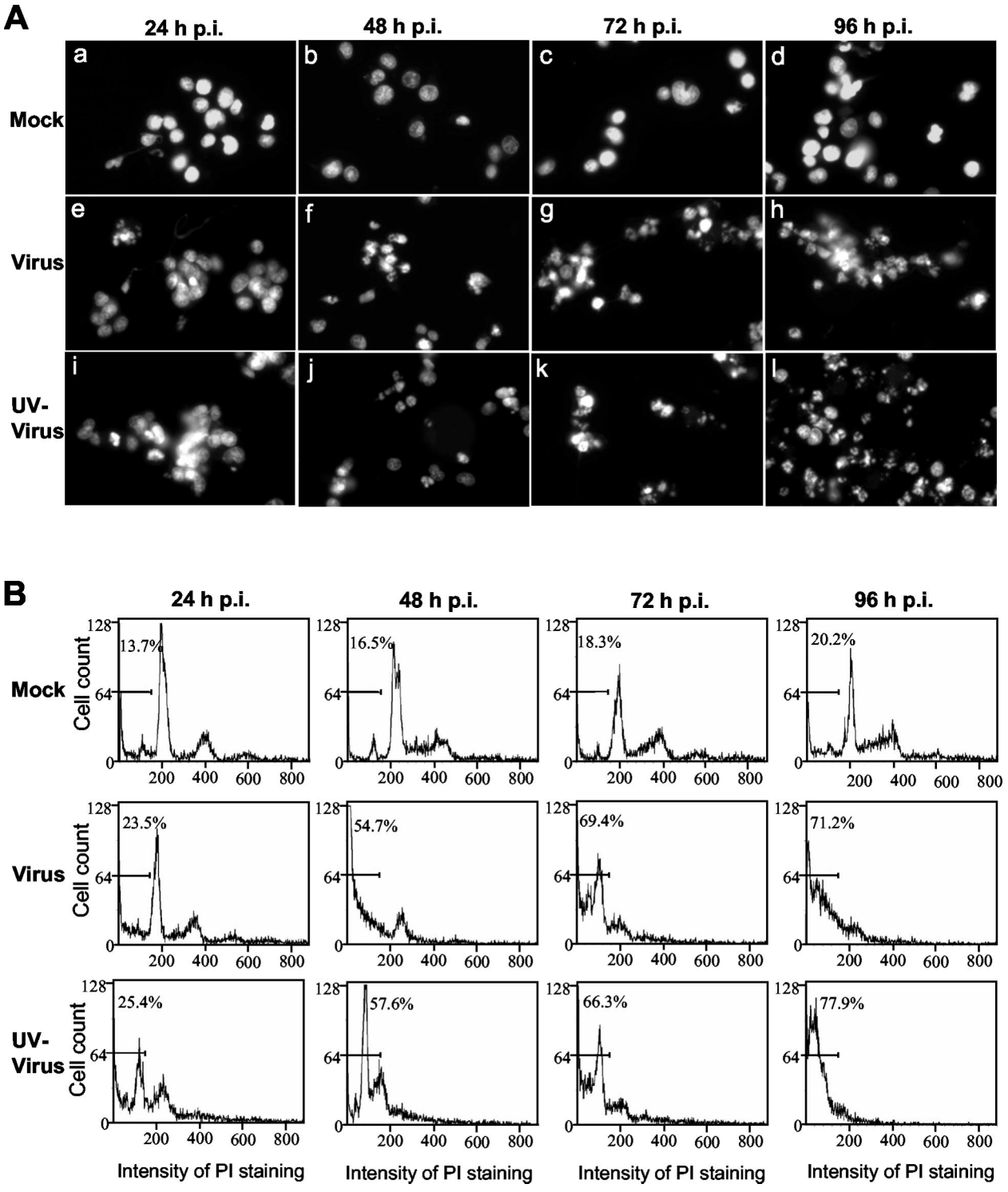

FIG. 3. MHV-induced apoptosis of mature rat oligodendrocytes. Mature oligodendrocytes were mock infected (Mock) or infected with MHV-JHM at an MOI of 10 (Virus) or with UV-inactivated MHV-JHM at an equivalent MOI (UV-Virus). At the indicated time points (hours) p.i., total cells were collected and stained with propidium iodide. A portion of the stained cells was subjected to microscopic examination (A), and the remainder was used for flow cytometric analysis (B). (A) Morphological characteristics of the nuclei of oligodendrocytes. All photographs were taken with a digital camera (MagnaFire) attached to a fluorescence microscope (Olympus IX-70) with the same magnification. (B) Results of flow cytometric analysis. The bar in each graph represents the sub-G_0/G_1 population of cells (indicated as a percentage) that have the lowest intensity of propidium iodide staining. Data are representative of at least three independent experiments.

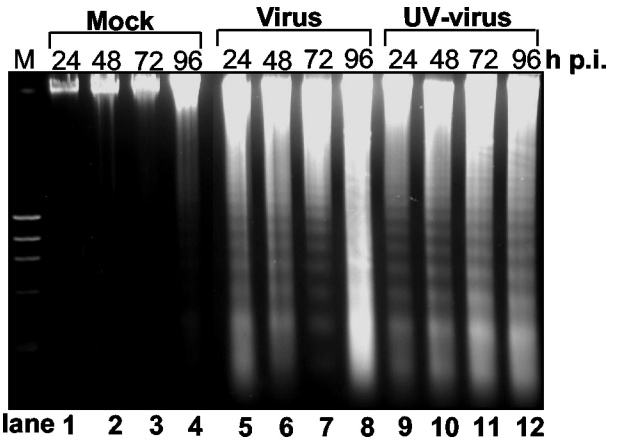

FIG. 4. DNA fragmentation of mature rat oligodendrocytes induced by MHV infection. Mature oligodendrocytes (5×10^5 cells) were mock infected (Mock; lanes 1 to 4) or infected with MHV-JHM at an MOI of 10 (Virus; lanes 5 to 8) or with UV-inactivated MHV-JHM at an equivalent MOI (UV-Virus; lanes 9 to 12). At the indicated time points p.i., total cells (including attached and detached cells) were collected and intracellular DNAs were isolated and analyzed by agarose gel (1.5%) electrophoresis using the DNA laddering kit as described in Materials and Methods. Data are representative of at least three independent experiments.

can still bind to the receptors of permissive cells and can be taken up by the cell; it cannot replicate in the cell, due to cross-linking of the viral genome. Therefore, the use of UV-inactivated virus for infection would separate the entry from postentry steps of the virus life cycle. Oligodendrocytes were infected with UV-inactivated MHV-JHM at a preirradiation MOI of 10, and apoptotic cells were determined by nuclear staining, flow cytometric analysis, and DNA fragmentation. Completeness of virus inactivation by UV irradiation was verified in indicator DBT cells, in which no CPE and negative-strand RNAs were detected by microscopic observation and reverse transcription-PCR, respectively, during the first 24 h p.i. (data not shown). As shown in Fig. 3 and 4, UV inactivation did not affect the apoptosis-inducing ability of the virus, as evidenced by the three criteria (the appearance of apoptotic bodies, increased number of sub-G_0/G_1-phase cells, and DNA fragmentation) from 24 to 96 h p.i., compared with the response in mock-infected cells (Fig. 3, compare UV-virus panels with mock panels; Fig. 4, compare lanes 9 to 12 with lanes 1 to 4). The extent of apoptosis was indistinguishable in oligodendrocytes infected with UV-irradiated virus and with live virus by the three criteria (compare virus panels with UV-virus panels in Fig. 3 and compare lanes 9 to 12 with lanes 5 to 8 in Fig. 4). These results demonstrate that viral RNA synthesis and subsequent steps in the virus life cycle are not required for the induction of apoptosis in oligodendrocytes. We thus conclude that oligodendrocyte apoptosis is triggered by MHV infection during early steps of the virus life cycle which are prior to viral RNA synthesis.

Virus-cell fusion during entry triggers the apoptosis in cultured oligodendrocytes. Since the above results identified the early steps of the infection process in the induction of apoptosis, we wanted to determine further the involvement of specific steps. The early steps of the virus life cycle include virus attachment to cell receptor, endocytosis, fusion between viral envelope and cytoplasmic or endosomal membranes, and separation of nucleocapsid protein from the viral RNA genome. For viruses that enter into cells via the endocytic pathway, a common approach to block virus uncoating is to raise the pH in the endosome by lysosomotropic agents. However, most MHV strains enter cells through both cell surface and endosomal membranes following endocytosis (33). Thus, treatment of cells with lysosomotropic agents does not block virus infection. To circumvent this problem, we used a mutant MHV, OBLV60, which is derived from the parental JHM strain and which has been shown to enter cells at acidic pH. Treatment of cells with ammonium chloride and chloroquine significantly inhibited OBLV60 infectivity and virus-induced cell fusion (15). Oligodendrocytes were treated with 50 mM ammonium chloride or 25 μM chloroquine at 1 h prior to virus infection and were infected with sucrose gradient-purified OBLV60 at an MOI of 10. At 1 h p.i., NH_4Cl or chloroquine was added to the medium and was present throughout the 72-h period p.i. Treated cells were then subjected to analysis of apoptosis. Treated and mock-infected cells were used as negative controls for determining any nonspecific effect of NH_4Cl and chloroquine on apoptosis. As shown in Fig. 5A, approximately 36 to 38% of the infected oligodendrocytes were in the sub-G_0/G_1 phase in the presence of NH_4Cl or chloroquine, whereas approximately 78% of the infected cells shifted to sub-G_0/G_1 phase in the absence of the drugs, indicating that both NH_4Cl and chloroquine are capable of inhibiting MHV-OBLV60-induced apoptosis. Figure 5B also shows an inhibitory effect of NH_4Cl or chloroquine on DNA fragmentation induced by OBLV60 infection. NH_4Cl or chloroquine by itself did not have a significant cytotoxic effect on oligodendrocytes at these concentrations, although the percentages of sub-G_0/G_1 cells were higher in treated cells than in untreated cells. As a control, a parallel experiment with wild-type MHV-JHM was performed. As expected, treatment of cells with NH_4Cl and chloroquine did not have a significant effect on the ability of wild-type MHV-JHM in inducing apoptosis (Fig. 5A and C). As an alternative approach to verify this finding, we used bafilomycin A1, a specific inhibitor of the vacuolar proton pump ATPase, which is required for acidification of the endosome. Inhibition of the proton pump would effectively block virus-cell fusion and uncoating via the endocytic pathway. As expected, bafilomycin A1 treatment inhibited the apoptosis induced by OBLV60 but not by wild-type MHV-JHM (Fig. 5). Taken together, these results demonstrate that fusion between viral envelope and endosomal membranes during OBLV60 uncoating is involved in the induction of apoptosis in oligodendrocytes. By extrapolating these data from the mutant OBLV60, we conclude that fusion between viral envelope and cytoplasmic and endosomal membranes during wild-type MHV infection triggers the apoptotic signaling cascade in oligodendrocytes.

MHV-induced apoptosis in cultured oligodendrocytes is caspase dependent. To determine whether MHV-induced apoptosis in oligodendrocytes is caspase dependent, we studied the effect of the broad-range caspases inhibitor Z-VAD-fmk on MHV-induced apoptosis. Oligodendrocytes were infected with purified MHV-JHM at an MOI of 10. At 1 h p.i., cells were treated with the caspase inhibitor at 80 μM, which has

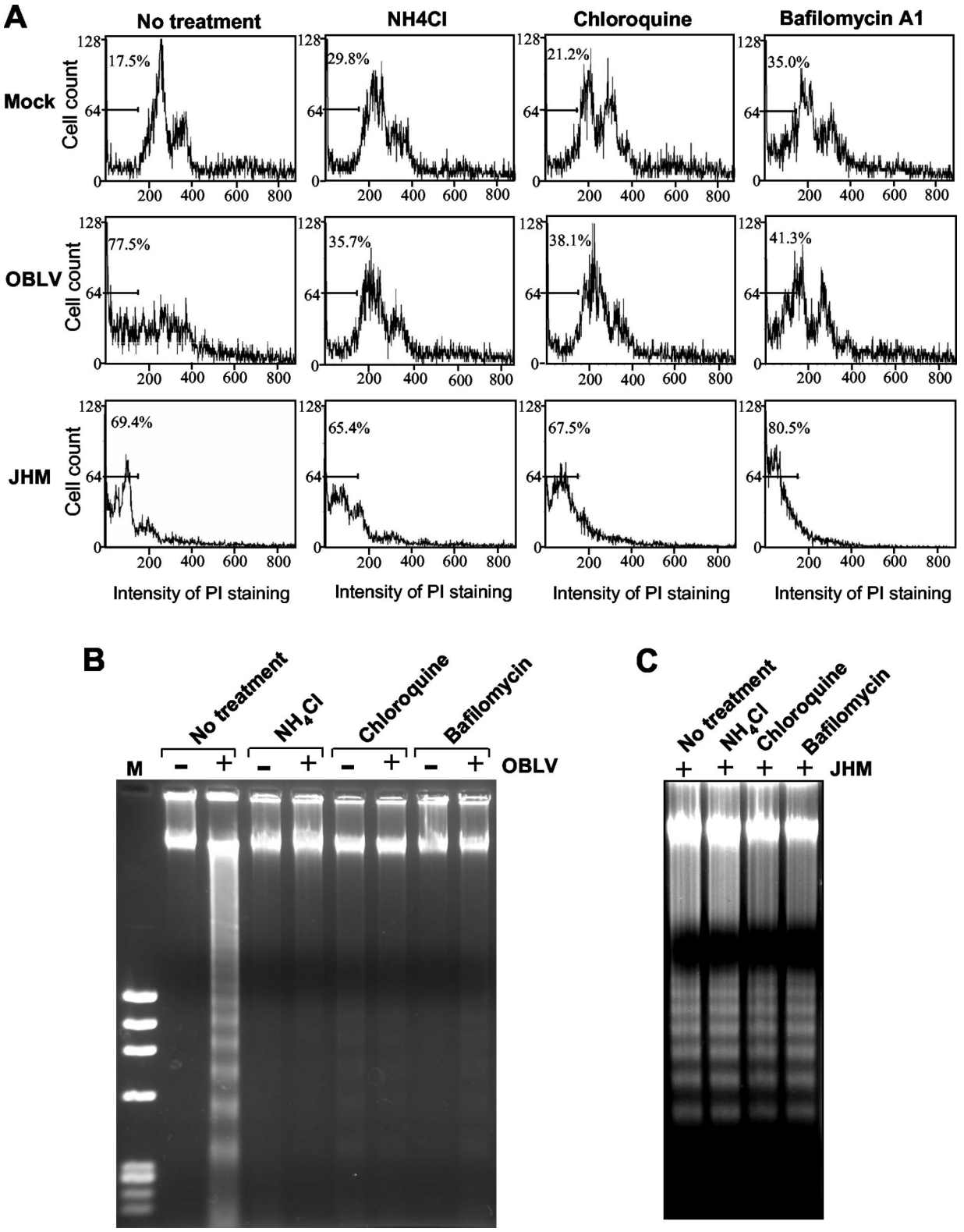

FIG. 5. Fusion between viral envelope and cell membranes during viral entry triggers a cellular apoptotic response. Mature oligodendrocytes were treated with NH_4Cl (50 mM), chloroquine (25 μM), or bafilomycin A1 (100 nM) as indicated at the top of each graph at 1 h prior to virus infection. Nontreated cells (no treatment) were used as a negative control. Following the treatment, cells were infected with sucrose gradient-purified MHV mutant OBLV60 or wild-type JHM at an MOI of 10. Mock-infected (Mock) cells were used for comparison and for determining the effects of the drugs on cell viability. At 72 h p.i., total cells (including attached and detached cells) were collected. One set of the cells was stained with propidium iodide and was subjected to flow cytometric analysis (A), and the other set was used for DNA fragmentation analysis (B and C). (A) Results of flow cytometric analysis. The bar in each graph represents the sub-G_0/G_1 population of cells (indicated as a percentage) that have the lowest intensity of propidium iodide staining. (B and C) DNA fragmentation analysis. Intracellular DNAs were isolated and analyzed by agarose gel (1.5%) electrophoresis using the DNA laddering kit as described in Materials and Methods. −, mock-infected cells; +, cells infected with OBLV60 (B) or with wild-type JHM (C). M, phiX DNA molecular weight marker. Data are representative of at least three independent experiments.

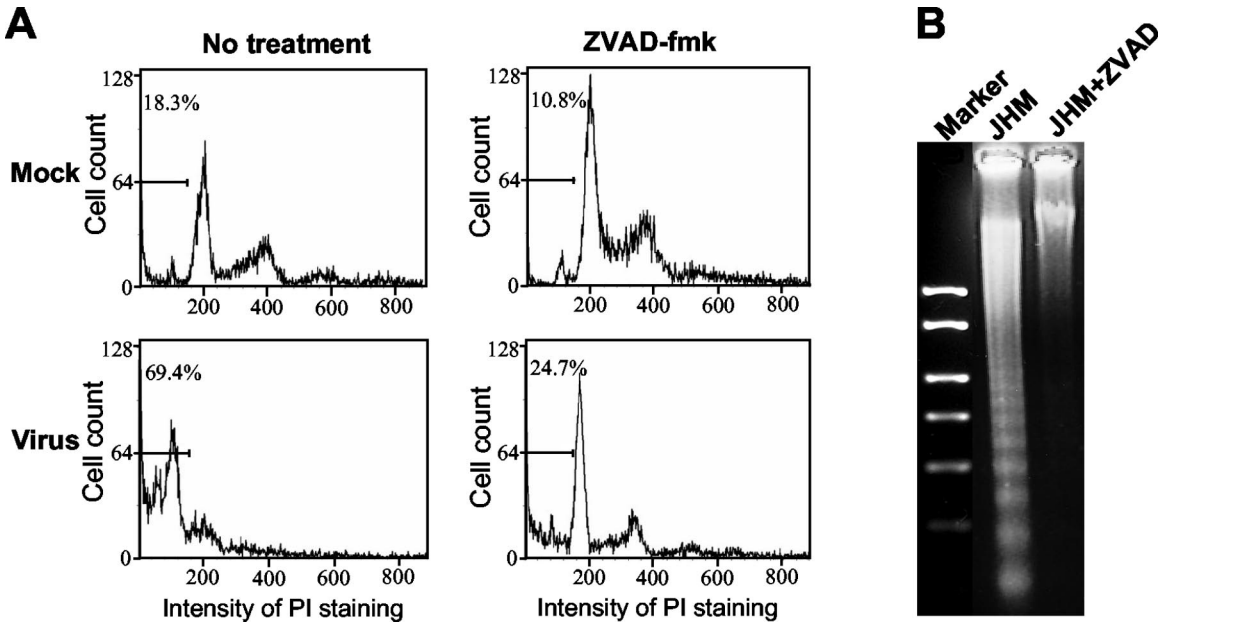

FIG. 6. MHV-induced oligodendrocyte apoptosis is caspase dependent. Mature oligodendrocytes were infected with MHV-JHM at an MOI of 10 or mock infected as a control. At 1 h p.i., cells were treated with the pan-caspase inhibitor Z-VAD-fmk (80 μM) or went without treatment. At 72 h p.i., total cells (including attached and detached cells) were collected. One set of the cells was stained with propidium iodide and subjected to flow cytometric analysis (A), and the other set was used for DNA fragmentation analysis (B). (A) Results of flow cytometric analysis. The bar in each graph represents the sub-G_0/G_1 population of cells (indicated as a percentage) that have the lowest intensity of propidium iodide (PI) staining. (B) DNA fragmentation analysis. Intracellular DNAs were isolated and analyzed by agarose gel (1.5%) electrophoresis using the DNA laddering kit as described in Materials and Methods. Data are representative of at least three independent experiments.

been shown to inhibit caspases completely in cultured mammalian cells (40) and which did not exhibit a toxic effect on oligodendrocytes as demonstrated in a cell viability assay (data not shown). At 72 h p.i., cells were stained with propidium iodide and subjected to flow cytometric analysis; cellular DNAs were isolated and used for DNA fragmentation analysis. As shown in Fig. 6A, a substantial number of infected cells (69.4%) were in sub-G_0/G_1 phase in the absence of the caspase inhibitor. In contrast, only 24.7% of the infected cells remained in sub-G_0/G_1 phase in the presence of the inhibitor, which was similar to the result in uninfected cells (18.3% in sub-G_0/G_1 phase). An inhibitory effect of the pan-caspase inhibitor on MHV-induced DNA fragmentation was also evident (Fig. 6B). Thus, MHV-induced apoptosis is caspase dependent.

DISCUSSION

A recent study has shown that MHV strain A59 induced CNS demyelination in RAG1 knockout mice, B-cell-deficient mice, and in mice that lack complement activity, suggesting that neither T cells nor B cells are required for CNS demyelination in mice infected with MHV-A59 (29, 30). This finding led us to hypothesize that MHV-induced acute demyelination may result from direct viral killing of oligodendrocytes and/or indirect destruction by inflammatory molecules secreted from CNS resident and infiltrated cells. While apoptotic oligodendrocytes have been identified in sections of brains and spinal cords of rats and mice infected with neurotropic MHV strains JHM and A59 (2, 39, 48), to date there is no direct evidence showing that MHV can directly induce oligodendrocyte apoptosis. This question cannot be unequivocally addressed in vivo (in animals) because of the complexity of the CNS and the presence of the host immune system. In the present study, we have addressed this question by establishing an in vitro cell culture system that is devoid of the host immune response. We showed that, under defined culture conditions, CG-4 progenitor cells differentiate into oligodendrocytes that resemble primary oligodendrocytes morphologically and phenotypically (28) (Fig. 1). Using these in vitro-differentiated oligodendrocytes, we were able to demonstrate that mature oligodendrocytes are susceptible to MHV infection as evidenced by the internalization of radiolabeled virions into the cells (Fig. 2B). However, mature oligodendrocytes do not support productive viral replication, since infectious virus titers decreased continuously from days 1 to 4 p.i. (Fig. 2). These results are in agreement with those obtained from MHV-JHM-infected, primary rat oligodendrocytes (36). Dales and coworkers have shown that primary rat oligodendrocytes are susceptible to MHV-JHM infection only for a short period of time during differentiation; once fully differentiated, they become resistant to MHV infection, suggesting that the susceptibility of oligodendrocytes to MHV infection is developmentally controlled (36). Subsequently, they found that the expression of the R1 subunit of protein kinase 1 is upregulated following treatment of progenitor cells with cyclic AMP, an inducer of oligodendrocyte maturation; overexpression of R1 inhibits an endosomal phosphoprotein phosphatase activity, which correlates with an inhibition of the dephosphorylation of viral nucleocapsid protein as well as viral production (22). Further, transfection of viral genomic RNA into mature oligodendrocytes allows viral production. It has been thus suggested that the

resistance of mature oligodendrocytes to MHV infection is restricted at the uncoating stage following viral entry (22). Our results from the virus plaque assay and internalization assay are consistent with this interpretation.

In addition, we detected viral antigens in less than 1% of the cells in the mature oligodendrocyte culture when using a specific antibody to the viral N protein in an immunofluorescence assay, even though all cells were presumably infected with the virus (at an MOI of 10 [Fig. 2D]). This suggests that the few virus replicating cells are either undifferentiated progenitor cells or differentiated astrocytes, which is consistent with the findings that less than 2% of the CG-4 progenitor cells did not become mature oligodendrocytes after differentiation (Fig. 1 and reference 28), although their identity was not determined directly. These results support the conclusion that mature oligodendrocytes do not support productive virus replication. However, this conclusion does not rule out the possibility that these mature oligodendrocytes can support low-level, nonproductive virus replication or become persistently infected with MHV, which could be below the limit of the immunofluorescence detection. Such a possibility remains to be further examined. Nevertheless, our finding that only a small percentage of the cells in a given oligodendrocyte culture support productive viral replication may explain why the virus titer was increased slightly ($\approx$1 $\log_{10}$ PFU/ml) following the eclipse period and why a small number of infectious viruses ($\approx$2 $\log_{10}$ PFU/ml) were consistently recovered from the culture by day 4 p.i.

Despite the finding that mature oligodendrocytes do not support productive MHV replication (Fig. 2), apoptosis is readily detected in oligodendrocytes as early as 24 h p.i. Using nucleic acid staining, flow cytometry, and DNA fragmentation analysis, we have unequivocally established in vitro that MHV infection can directly induce apoptosis in mature rat oligodendrocytes in the absence of other CNS cells and host immune cells (Fig. 3 and 4). Of note, because the viral inoculum is purified via sucrose gradient ultracentrifugation and is devoid of any soluble factors that might be secreted from cells during viral propagation, the observed apoptotic effect must be mediated directly by the viral inoculum. To provide evidence in support of this conclusion, we tested the possibility that any soluble factors that are secreted from virus-infected oligodendrocytes might act upon oligodendrocytes to induce apoptosis secondarily. Mature oligodendrocytes were infected with purified MHV. At 24 h p.i., culture medium was collected and clarified to deplete existing virions by ultracentrifugation. The supernatant was then added to the fresh, mature oligodendrocyte culture. If the supernatant contains apoptotic inducers, then incubation with the supernatant would result in oligodendrocyte apoptosis. As expected, neither the number of apoptotic cells nor DNA fragmentation was detectably increased in oligodendrocytes cultured with the virus-infected supernatant compared with results in oligodendrocytes cultured with normal medium from days 1 to 4 p.i. (data not shown). Thus, oligodendrocyte apoptosis is the direct result of MHV infection.

In the present study, we have shown that oligodendrocyte apoptosis is mediated by virus entry into cells and does not require virus replication, as demonstrated by the ability of inducing apoptosis by UV-inactivated virus. Furthermore, treatment of oligodendrocytes with the lysosomotropic agents ammonium chloride and chloroquine as well as bafilomycin A1 (an inhibitor of the vacuolar proton pump ATPase), all of which block the acidification of the endosome and consequently the fusion between endosomal membranes and the viral envelope, also prevented OBLV60-induced apoptosis (Fig. 5). These results strongly suggest that virion attachment to the cell receptor, the first step in initiating virus infection, is not sufficient, though it is necessary, for apoptosis induction; instead, the fusion process (between viral envelope and cell membrane), an obligate uncoating step of the viral infectious cycle subsequent to virus attachment, triggers the apoptotic cascade. How MHV-cell fusion induces apoptosis remains an interesting subject for future study. Our results suggest that the viral spike glycoprotein is likely responsible for triggering the cellular apoptotic response during fusion with cell membranes. Alternatively, the M and E proteins in the viral envelope may also participate in the signaling event. Overexpression of the E protein by a recombinant vaccinia virus results in apoptosis of DBT cells (1). A number of viruses, including avian leukosis virus (4), bovine herpesvirus 1 (16), vaccinia virus (37), reovirus (43), and Sindbis virus (21), have been shown to be capable of inducing apoptosis in the absence of virus replication, although the mechanisms by which these viruses cause apoptotic cell death have not been definitely determined. For reovirus, a nonenveloped RNA virus, apoptosis is mediated by virion disassembly in the endosome, since treatment of cells with ammonium chloride, which blocks virion disassembly into the infectious subviral particle in the endosome, completely inhibits reovirus-induced apoptosis (7). Moreover, it appears that reovirus receptors do not initiate the signaling events that induce apoptosis from the cell surface, although viral attachment to the receptors is required for the endocytosis and apoptotic induction (7). Similarly, for the enveloped Sindbis virus, apoptosis is triggered by events that occur during cell entry subsequent to attachment (20, 21). Inhibitors of endosomal acidification, which block Sindbis virus fusion with endosomal membranes, also block virus-induced apoptosis (21). Further, interaction of Sindbis virus glycoproteins E1 and E2 with endosomal membranes results in activation of sphingomyelinases and the subsequent accumulation of ceramide, which has been postulated to mediate the apoptotic response following Sindbis virus infection (20). These findings indicate that the initiation of Sindbis virus-induced apoptosis is triggered by fusion of the viral envelope with endosomal membranes. Whether MHV-induced oligodendrocyte apoptosis is also mediated by the viral fusogenic envelope S protein and/or other envelope proteins through the activation of sphingomyelinase and ceramides during fusion of viral envelope with cell membranes, as shown in Sindbis virus-induced apoptosis, remains to be seen.

Our present finding that MHV induces apoptosis in oligodendrocytes raises the possibility that apoptosis is one of the mechanisms of MHV-induced CNS demyelination seen in animals. In support of this hypothesis is the observation that apoptotic oligodendrocytes are found in the vicinity of demyelinating lesions in rats and mice infected with MHV strains (2, 39, 48), although it has been reported that the distribution of apoptotic cells correlated with macrophage infiltration rather than apoptosis (48). Based on the results presented here and previous data from others, the following model regarding the pathogenesis of MHV-induced CNS demyelination is pro-

posed. During acute and persistent infection, MHV directly attacks oligodendrocytes and triggers a cellular apoptotic response at the site of fusion between the viral envelope and cell membranes during virus entry into cells. Once the virus has entered the cells, it does not undergo replication due to a block in uncoating. Such "suicide bombing" by the virus results in destruction of oligodendrocytes and consequently elimination of infectious virus. This may explain why little or no colabeling of terminal deoxynucleotidyltransferase-mediated dUTP-biotin nick end labeling-positive and virus antigen-positive oligodendrocytes is found in the demyelinating lesions of the brain and spinal cord of MHV-infected mice (39, 48). Consequently, the demyelinating lesions are focal and localized due to the inability of virus production and spread from primary infected oligodendrocytes. These lesions may or may not be recognized in CNS sections under microscopic observation. Massive demyelination likely requires secondary attacks by the virus and/or by molecules that are secreted from virus-infected resident CNS cells or cells of the immune system that have infiltrated into the CNS during the course of infection.

In conclusion, our results unequivocally demonstrate for the first time that MHV directly kills oligodendrocytes by inducing apoptosis. Moreover, the apoptosis is mediated by fusion of the viral envelope with cell membranes subsequent to virus attachment through caspase-dependent pathways and does not require virus replication.

ACKNOWLEDGMENTS

This work was supported by a grant from the National Institutes of Health (AI 47188).

We thank Michael Buchmeier (Scripps Research Institute), Paul Drew (University of Arkansas for Medical Sciences), and Stephen Stohlman (University of Southern California, Los Angeles, Calif.) for kindly providing the MHV mutant OBLV60, CG-4 cells, and the MAb to MHV N protein, respectively.

REFERENCES

1. **An, S., C. J. Chen, X. Yu, J. L. Leibowitz, and S. Makino.** 1999. Induction of apoptosis in murine coronavirus-infected cultured cells and demonstration of E protein as an apoptosis inducer. J. Virol. **73:**7853–7859.
2. **Barac-Latas, V., G. Suchanek, H. Breitschopf, A. Stuehler, H. Wege, and H. Lassmann.** 1997. Patterns of oligodendrocytes pathology in coronavirus-induced subacute demyelination encephalomyelitis in the Lewis rat. Glia **19:**1–12.
3. **Beushausen, S., S. Narindrasorasak, B. D. Sanwal, and S. Dales.** 1987. In vivo and in vitro models of demyelinating disease: activation of the adenylate cyclase system influences JHM virus expression in explanted rat oligodendrocytes. J. Virol. **61:**3795–3803.
4. **Brojatsch, J., J. Naughton, M. M. Rolls, K. Zingler, and J. A. Young.** 1996. CAR1, a TNFR-related protein, is a cellular receptor for cytopathic avian leukosis-sarcoma viruses and mediates apoptosis. Cell **87:**845–855.
5. **Chen, X., V. Zachar, M. Zdravkovic, M. Guo, P. Ebbesen, and X. Liu.** 1997. Role of the Fas/Fas ligand pathway in apoptotic cell death induced by the human T cell lymphotropic virus type I Tax transactivator. J. Gen. Virol. **78:**3277–3385.
6. **Collins, A. R., R. L. Knobler, H. Powell, and M. J. Buchmeier.** 1982. Monoclonal antibodies to murine hepatitis virus-4 (strain JHM) define the viral glycoprotein responsible for attachment and cell-cell fusion. Virology **119:** 358–371.
7. **Connolly, J. L., and T. S. Dermody.** 2002. Virion disassembly is required for apoptosis induced by reovirus. J. Virol. **76:**1632–1641.
8. **Corallini, A., R. Sampaolesi, L. Possati, M. Merlin, P. Bagnarelli, C. Piola, M. Fabris, M. A. Menegatti, S. Talevi, D. Gibellini, et al.** 2002. Inhibition of HIV-1 Tat activity correlates with down-regulation of bcl-2 and results in reduction of angiogenesis and oncogenicity. Virology **299:**1–7.
9. **Dandekar, A. A., and S. Perlman.** 2002. Virus-induced demyelination in nude mice is mediated by gamma delta T cells. Am. J. Pathol. **161:**1255–1263.
10. **Das Sarma, J., L. Fu, J. C. Tsai, S. R. Weiss, and E. Lavi.** 2000. Demyelination determinants map to the spike glycoprotein gene of coronavirus mouse hepatitis virus. J. Virol. **74:**9206–9213.
11. **Duerksen-Hughes, P., W. S. Wold, and L. R. Gooding.** 1989. Adenovirus E1A renders infected cells sensitive to cytolysis by tumor necrosis factor. J. Immunol. **143:**4193–4200.
12. **Duerksen-Hughes, P. J., T. W. Hermiston, W. S. Wold, and L. R. Gooding.** 1991. The amino-terminal portion of DC1 of the adenovirus E1A proteins is required to induce susceptibility to tumor necrosis factor cytolysis in adenovirus-infected mouse cells. J. Virol. **65:**1236–1244.
13. **Dveksler, G. S., M. N. Pensiero, C. B. Cardellichio, R. K. Williams, G. Jiang, K. V. Holmes, and C. W. Dieffenbach.** 1991. Cloning of the mouse hepatitis virus (MHV) receptor: expression in human and hamster cell lines confers susceptibility to MHV. J. Virol. **65:**6881–6891.
14. **Fleming, J. O., F. I. Wang, M. D. Trousdale, D. R. Hinton, and S. A. Stohlman.** 1993. Interaction of immune and central nervous systems: contribution of anti-viral Thy-1^+ cells to demyelination induced by coronavirus JHM. Regul. Immunol. **5:**37–43.
15. **Gallagher, T. M., C. Escarmis, and M. J. Buchmeier.** 1991. Alteration of the pH dependence of coronavirus-induced cell fusion: effect of mutations in the spike glycoprotein. J. Virol. **65:**1916–1928.
16. **Hanon, E., G. Meyer, A. Vanderplasschen, C. Dessy-Doize, E. Thiry, and P. P. Pastoret.** 1998. Attachment but not penetration of bovine herpesvirus 1 is necessary to induce apoptosis in target cells. J. Virol. **72:**7638–7641.
17. **Hirano, N., K. Fujiwara, S. Hino, and M. Matumoto.** 1974. Replication and plaque formation of mouse hepatitis virus (MHV-2) in mouse cell line DBT culture. Arch. Gesamte Virusforsch. **44:**298–302.
18. **Hirano, N., K. Fujiwara, and M. Matumoto.** 1976. Mouse hepatitis virus (MHV-2). Plaque assay and propagation in mouse cell line DBT cells. Jpn. J. Microbiol. **20:**219–225.
19. **Houtman, J. J., and J. O. Fleming.** 1996. Dissociation of demyelination and viral clearance in congenitally immunodeficient mice infected with murine coronavirus JHM. J. Neurovirol. **2:**101–110.
20. **Jan, J. T., S. Chatterjee, and D. E. Griffin.** 2000. Sindbis virus entry into cells triggers apoptosis by activating sphingomyelinase, leading to the release of ceramide. J. Virol. **74:**6425–6432.
21. **Jan, J. T., and D. E. Griffin.** 1999. Induction of apoptosis by Sindbis virus occurs at cell entry and does not require virus replication. J. Virol. **73:**10296–10302.
22. **Kalicharran, K., D. Mohandas, G. Wilson, and S. Dales.** 1996. Regulation of the initiation of coronavirus JHM infection in primary oligodendrocytes and L-2 fibroblasts. Virology **225:**33–43.
23. **Knobler, R. L., M. Dubois-Dalcq, M. V. Haspel, A. P. Claysmith, P. W. Lampert, and M. B. Oldstone.** 1981. Selective localization of wild type and mutant mouse hepatitis virus (JHM strain) antigens in CNS tissue by fluorescence, light and electron microscopy. J. Neuroimmunol. **1:**81–92.
24. **Kooi, C., M. Cervin, and R. Anderson.** 1991. Differentiation of acid-pH-dependent and -nondependent entry pathways for mouse hepatitis virus. Virology **180:**108–119.
25. **Lai, M. M. C., and D. Cavanagh.** 1997. The molecular biology of coronaviruses. Adv. Virus Res. **48:**1–100.
26. **Lampert, P. W., J. K. Sims, and A. J. Kniazeff.** 1973. Mechanism of demyelination in JHM virus encephalomyelitis. Electron microscopic studies. Acta Neuropathol. (Berlin) **24:**76–85.
27. **Lavi, E., D. H. Gilden, M. K. Highkin, and S. R. Weiss.** 1984. Persistence of mouse hepatitis virus A59 RNA in a slow virus demyelinating infection in mice as detected by in situ hybridization. J. Virol. **51:**563–566.
28. **Louis, J. C., E. Magal, D. Muir, M. Manthorpe, and S. Varon.** 1992. CG-4, a new bipotential glial cell line from rat brain, is capable of differentiating in vitro into either mature oligodendrocytes or type-2 astrocytes. J. Neurosci. Res. **31:**193–204.
29. **Matthews, A. E., E. Lavi, S. R. Weiss, and Y. Paterson.** 2002. Neither B cells nor T cells are required for CNS demyelination in mice persistently infected with MHV-A59. J. Neurovirol. **8:**257–264.
30. **Matthews, A. E., S. R. Weiss, and Y. Paterson.** 2002. Murine hepatitis virus—a model for virus-induced CNS demyelination. J. Neurovirol. **8:**76–85.
31. **McNulty, S., M. Crouch, D. Smart, and M. Rumsby.** 2001. Differentiation of bipolar CG-4 line oligodendrocytes is associated with regulation of CREB, MAP kinase and PKC signaling pathways. Neurosci. Res. **41:**217–226.
32. **Miura, T. A., K. Morris, S. Ryan, J. L. Cook, and J. M. Routes.** 2003. Adenovirus E1A, not human papillomavirus E7, sensitizes tumor cells to lysis by macrophages through nitric oxide- and TNF-alpha-dependent mechanisms despite up-regulation of 70-kDa heat shock protein. J. Immunol. **170:**4119–4126.
33. **Nash, T. C., and M. J. Buchmeier.** 1997. Entry of mouse hepatitis virus into cells by endosomal and nonendosomal pathways. Virology **233:**1–8.
34. **Niemann, H., and H. D. Klenk.** 1981. Coronavirus glycoprotein E1, a new type of viral glycoprotein. J. Mol. Biol. **153:**993–1010.
35. **Nijhawan, D., N. Honarpour, and X. Wang.** 2000. Apoptosis in neural development and disease. Annu. Rev. Neurosci. **23:**73–87.
36. **Pasick, J. M., and S. Dales.** 1991. Infection by coronavirus JHM of rat neurons and oligodendrocyte-type-2 astrocyte lineage cells during distinct developmental stages. J. Virol. **65:**5013–5028.
37. **Ramsey-Ewing, A., and B. Moss.** 1998. Apoptosis induced by a post binding

step of vaccinia virus entry into Chinese hamster ovary cells. Virology **242:** 138–149.
38. **Roulston, A., R. Marcellus, and P. Branton.** 1999. Viruses and apoptosis. Annu. Rev. Microbiol. **53:**577–628.
39. **Schwartz, T., L. Fu, and E. Lavi.** 2001. Programmed cell death in MHV-induced demyelination. Adv. Exp. Med. Biol. **494:**163–167.
40. **Slee, E. A., H. Zhu, S. C. Chow, M. MacFarlane, D. W. Nicholson, and G. M. Cohen.** 1996. Benzyloxycarbonyl-Val-Ala-Asp (OMe) fluoromethylketone (Z-VAD.FMK) inhibits apoptosis by blocking the processing of CPP32. Biochem. J. **315:**21–24.
41. **Stohlman, S. A., and M. M. C. Lai.** 1979. Phosphoproteins of murine hepatitis viruses. J. Virol. **32:**672–675.
42. **Sturman, L. S., C. S. Ricard, and K. V. Holmes.** 1990. Conformational change of the coronavirus peplomer glycoprotein at pH 8.0 and 37 degrees C correlates with virus aggregation and virus-induced cell fusion. J. Virol. **64:**3042–3050.
43. **Tyler, K. L., M. K. Squier, S. E. Rodgers, B. E. Schneider, S. M. Oberhaus, T. A. Grdina, J. J. Cohen, and T. S. Dermody.** 1995. Differences in the capacity of reovirus strains to induce apoptosis are determined by the viral attachment protein sigma 1. J. Virol. **69:**6972–6979.
44. **Van Dinter, S., and W. F. Flintoff.** 1987. Rat glial C6 cells are defective in murine coronavirus internalization. J. Gen. Virol. **68:**1677–1685.
45. **Vennema, H., G. J. Godeke, J. W. Rossen, W. F. Voorhout, M. C. Horzinek, D. J. Opstelten, and P. J. Rottier.** 1996. Nucleocapsid-independent assembly of coronavirus-like particles by co-expression of viral envelope protein genes. EMBO J. **15:**2020–2028.
46. **Wang, F. I., S. A. Stohlman, and J. O. Fleming.** 1990. Demyelination induced by murine hepatitis virus JHM strain (MHV-4) is immunologically mediated. J. Neuroimmunol. **30:**31–41.
47. **Williams, R. K., G. Jiang, and K. V. Holmes.** 1991. Receptor for mouse hepatitis virus is a member of the carcinoembryonic antigen family of glycoproteins. Proc. Natl. Acad. Sci. USA **88:**5533–5536.
48. **Wu, G. F., and S. Perlman.** 1999. Macrophage infiltration, but not apoptosis, is correlated with immune-mediated demyelination following murine infection with a neurotropic coronavirus. J. Virol. **73:**8771–8780.
49. **Wu, G. F., A. A. Dandekar, L. Pewe, and S. Perlman.** 2000. CD4 and CD8 T cells have redundant but not identical roles in virus-induced demyelination. J. Immunol. **165:**2278–2286.
50. **Wyllie, A. H.** 1980. Glucocorticoid-induced thymocyte apoptosis is associated with endogenous endonuclease activation. Nature **284:**555–556.
51. **Yokomori, K., L. R. Banner, and M. M. C. Lai.** 1991. Heterogeneity of gene expression of the hemagglutinin-esterase (HE) protein of murine coronaviruses. Virology **183:**647–657.
52. **Yokomori, K., N. La Monica, S. Makino, C. K. Shieh, and M. M. C. Lai.** 1989. Biosynthesis, structure, and biological activities of envelope protein gp65 of murine coronavirus. Virology **173:**683–691.
53. **Yokomori, K., and M. M. Lai.** 1992. Mouse hepatitis virus utilizes two carcinoembryonic antigens as alternative receptors. J. Virol. **66:**6194–6199.
54. **Yu, D. S., C. M. Hsu, W. H. Lee, S. Y. Chang, and C. P. Ma.** 1993. Flow cytometric DNA and cytomorphometric analysis in renal cell carcinoma: its correlation with histopathology and prognosis. J. Surg. Res. **55:**480–485.
55. **Yu, X., W. Bi, S. R. Weiss, and J. L. Leibowitz.** 1994. Mouse hepatitis virus gene 5b protein is a new virion envelope protein. Virology **202:**1018–1023.